Vol 5 (1) (2024)

Measurement, Control, and Automation

Website: https:// mca-journal.org

ISSN 1859-0551

Online Inductances Estimation of the Permanent Magnet Synchronous Machines based on Deep Learning and Recursive Least Square Algorithms

Bui Xuan Minh[1]*, Le Khac Thuy[1], Le Minh Kien[1], Nguyen Trung Kien[1], Nguyen Thanh Tien[1], Pham Xuan Phuong[1]

[1] *Le Quy Don Technical University, Ha Noi, Vietnam*
[*]*Corresponding author E-mail: minh.buixuan@ieee.org*

Abstract

This paper presents a novel method to identify in real time d- and q- axes inductances of the permanent magnet synchronous machines (PMSMs), which normally vary during the operation due to the saturation of the magnetic fields. The proposed method is based on the combination of deep learning and recursive least square algorithms. The deep learning model is trained offline to compensate the non-linearity effect of the voltage source inverter and the position measurement error, while the recursive least square algorithm is employed to estimate online d- and q- axes inductances based on the compensation d- and q- axes stator voltages, measured d- and q- axes stator currents and the operating speed. The proposed methods can overcome the problems associated with the existing model-based methods known as the effect of position measurement error and the unavailability of accurate information of the inverter. Extensive experimental studies were conducted to evaluate the estimation accuracy and the robustness of the proposed method in critical operating conditions including the variation of load torque, operating speed, and field-weakening condition.

Keywords*: PMSM, Online Parameter Identification, Deep Learning, Recursive Least Square.*

Symbols

Symbols	Units	Description
Ψ_m	Wb	Rotor flux linkage
R_s	Ω	Stator resistance
L_d, L_q	H	*d*- and *q*- axes stator inductance
i_d, i_q	A	*d*- and *q*- axes stator currents
v_d, v_q	V	*d*- and *q*- axes stator voltages
ω_{re}	Rad/s	Electrical angular speed of the rotor
θ_{re}	Rad/s	Electrical angular position of the rotor

Abbreviations

PMSM	Permanent Magnet Synchronous Machines
RLS	Recursive Least Square
ANN	Adaline Neural Network
FOC	Field Oriented Control
DTC	Direct Torque Control
MPC	Model Predictive Control

1. Introduction

Permanent magnet synchronous machines (PMSM) have been widely used in high-end applications, such as electric vehicles, wind-turbine generation, and robotics. The main advantages of these types of electric machines are known as high power density, high torque density and high control performance. So far, field-oriented control (FOC), direct torque control (DTC) and model predicted control (MPC) are the most popular control schemes for PMSMs. These control methods require accurate parameters of the machines including stator resistance, d- and q- axes inductances and the rotor flux linkages. Among these four parameters, stator resistance and rotor fluxing linkage do not change significantly during the operation; in contrast, d- and q- axes inductances are normally varied according to the variation of the load torque due to the saturation of the magnetic field [1]. So far, the techniques to identify machine parameters can be classified as offline and online. The offline methods are based on running of the rotor at a certain speed [2] or locking the rotor at a specific position [3], applying the test signals and then processing the current or voltage response to identify the machine parameters. These methods exhibit the weakness of requiring additional hardware for producing test signals and the mechanical systems to clamp or run the rotor shaft.

Received: 03 November 2023; Accepted: 13 March 2024.

Online methods in contrast have been proposed to estimate the machine parameters during the normal operation of the control system. Most of the existing online methods are based on the dynamic model of the machine on the synchronous reference frame (dq), and the utilization of advanced control theories, such as recursive least square [4-7], Kalman filters [8-10], model reference adaptive system [11-13], Adaline neural network [14, 15]. These methods are based on the measurement of the d- axis and q-axis stator current, rotor speed and the estimated d- and q- stator voltages. Normally, the phase voltages are noisy, pulsated and not available to calculate the d- and q- axes stator voltages. Therefore, these voltages are taken as output voltage of the corresponding d- and q- axes current controller in FOC algorithm [16]. However, due to the non-linearity of the voltage source inverter, there is a deviation of the measured and the actual d- and q- axes voltages. Consequently, the compensation of the non-linearity of the inverter must be implemented. The compensation scheme requires accurate information of the inverter including characteristics of the main switches and the freewheel diodes, which are not normally available in most of the commercial voltage source inverters. In addition, the delay of the inverter and the digital sampling also produce the error between the actual and the measured rotor position [17]. This hinders the compensation implementation and the application of the aforementioned methods. The method shown in [18] has shown the merits in identifying four machine parameters by using the feedforward neural network; however, the experimental verification has not been published.

In order to solve the challenges of the model based online methods, the authors in [19, 20] have presented a method to estimate the d- and q- axes inductances of the IPMSM based on the measurement of the slopes of the phase current, together with the DC bus voltage during excitation of every voltage and zero voltage vector in a pule width modulation (PWM) cycle. Although these approaches have shown high estimation accuracy, it requires high-bandwidth current sensors, high-speed analog to digital converter (ADC) and high-computational digital signal processors (DSPs), such as Field Programmable Gate Array (FPGA). This is still a challenge for the application of this method in the drive systems with low computational capability.

Therefore, this paper proposes a novel method to estimate the machine inductances in real-time and overcome the weakness of the existing online model-based methods due to the effect of noise and the non-linearity of the voltage source inverter. The proposed parameter estimation method is based on the combination of deep learning and recursive least square algorithm. The deep learning neural network model was trained offline using experimental data in order to compensate the measured d- and q- voltages. On the other hand, the recursive least square algorithm was utilized to estimate d- and q- axes inductances of the PMSM. The rest of this paper is organized as follows: the second section presents the details of the proposed online parameter identification method, while the third section presents the experimental validation of the proposed approach. Finally, the conclusion is presented in the fourth section.

2. Proposed online parameters identification method.

2.1. PMSM dynamic model

The dynamic model of the PMSM on the actual d-q reference frame can be expressed as followed:

$$\begin{aligned} v_d &= R_s i_d + L_d \frac{di_d}{dt} - \omega_{re} L_q i_q \\ v_q &= R_s i_q + L_q \frac{di_q}{dt} + \omega_{re}(L_d i_d + \psi_m) \end{aligned} \quad (1)$$

where $v_{d,q}$ and $i_{d,q}$ are the d- and q- axes stator voltage and current, respectively; $L_{d,q}$ are d- and q- axes inductances. ω_{re} is the actual electrical rotor speed; R_s and ψ_m are the stator winding resistance and the rotor flux linkage, respectively.

The dynamic model of the PMSM on the estimated d-q reference can be represented as [17]:

$$\begin{aligned} \hat{v}_d &= R_s \hat{\imath}_d + L_d \tfrac{d\hat{\imath}_d}{dt} - \hat{\omega}_{re} L_q \hat{\imath}_q + \hat{E}_{ex} sin\tilde{\theta}_{re} \\ \hat{v}_q &= R_s \hat{\imath}_q + L_q \tfrac{d\hat{\imath}_q}{dt} + \hat{\omega}_{re} L_d \hat{\imath}_d + \hat{E}_{ex} cos\tilde{\theta}_{re} \\ \hat{E}_{ex} &= \hat{\omega}_{re}\psi_m + \hat{\omega}_{re}(L_d - L_q)\hat{\imath}_d - (L_d - L_q)(\frac{d\hat{\imath}_q}{dt}) \end{aligned} \quad (2)$$

where the accent symbol "^" indicates the quantities on the estimated d-q reference frame $(\hat{d}, \hat{q})$; $\tilde{\theta}_{re} = \hat{\theta}_{re} - \theta_{re}$ is the error between the measured $(\hat{\theta}_{re})$ and the actual electrical rotor position (θ_{re}).

2.2. Non-linearity effect of the voltage source inverter

Usually, three phase voltages of the machine are not available for estimating the d- and q- axes stator voltages as shown in equation (2). Therefore, the reference d- and q- axes stator voltages as the output of the corresponding d- and q-axes current controllers are often used as the input of the conventional model-based control and parameter identification methods. However, due to the effect of the deadtime, the voltage drop on the main switches and free wheel diodes of the two level three phase inverter, there exists the deviation of the measured and the actual d- and q- axes voltages as followed [8]:

$$\begin{pmatrix} \Delta\hat{v}_d \\ \Delta\hat{v}_q \end{pmatrix} = U_{DB} P(\hat{\theta}_{re}) \big(\text{sign}(i_a), \text{sign}(i_b), \text{sign}(i_c)\big)^T \quad (3)$$

where:

$$\text{sign}(i_j) = \begin{cases} 1 \; if \; i_j \geq 0 \\ -1 \; if \; i_j < 0 \end{cases} \text{ with } j = a, b, c \quad (4)$$

$$P(\hat{\theta}_{re}) = \frac{2}{3}\begin{pmatrix} \cos(\hat{\theta}_{re}) & \cos(\hat{\theta}_{re} - 2\pi/3) & \cos(\hat{\theta}_{re} + 2\pi/3) \\ \sin(\hat{\theta}_{re}) & \sin(\hat{\theta}_{re} - 2\pi/3) & \sin(\hat{\theta}_{re} + 2\pi/3) \\ 1/2 & 1/2 & 1/2 \end{pmatrix} \quad (5)$$

$$U_{DB} = \frac{T_{DB} + T_{on} - T_{off}}{T_{PWM}}(V_{DC} - V_S + V_D) + \frac{V_S + V_D}{2} \quad (6)$$

where T_{DB}, T_{on}, T_{off} and T_{PWM} are the dead time of the voltage source inverter, turning on time, turning off time of the main switch and the PWM period, respectively; V_{DC} is the DC bus voltage; V_S and V_D are the voltage drop on the main switch and the free wheel diode, respectively.
By combining the effects of the position measurement error and the non-linearity of the inverter, the dynamic model of PMSM on the estimated d-q reference frame can be presented as follows:

$$\begin{aligned} \hat{v}_d^* + \Delta\hat{v}_d &= R_s\hat{\imath}_d + L_d\frac{d\hat{\imath}_d}{dt} - \hat{\omega}_{re}L_q\hat{\imath}_q + \hat{E}_{ex}sin\tilde{\theta}_{re} \\ \hat{v}_q^* + \Delta\hat{v}_q &= R_s\hat{\imath}_q + L_q\frac{d\hat{\imath}_q}{dt} + \hat{\omega}_{re}L_d\hat{\imath}_d + \\ &\quad + \hat{E}_{ex}\left(1 - 2\sin^2\left(0.5\tilde{\theta}_{re}\right)\right) \end{aligned} \tag{7}$$

where $\hat{v}_d^*$ and $\hat{v}_q^*$ are the measured voltages at the output of the d- and q- axes current controllers, respectively.
Define the compensated d-and q- axes stator voltages on the estimated d-q reference frame:

$$\begin{aligned} \hat{v}_{d,comp} &= \Delta\hat{v}_d - \hat{E}_{ex}sin\tilde{\theta}_{re} \\ \hat{v}_{q,comp} &= \Delta\hat{v}_q + 2\hat{E}_{ex}\sin^2\left(0.5\tilde{\theta}_{re}\right) \end{aligned} \tag{8}$$

Equations (7) can be rewritten as:

$$\begin{aligned} \hat{v}_d^* + \hat{v}_{d,comp} &= R_s\hat{\imath}_d + L_d\frac{d\hat{\imath}_d}{dt} - \hat{\omega}_{re}L_q\hat{\imath}_q \\ \hat{v}_q^* + \hat{v}_{q,comp} &= R_s\hat{\imath}_q + L_q\frac{d\hat{\imath}_q}{dt} + \hat{\omega}_{re}(L_d\hat{\imath}_d + \psi_m) \end{aligned} \tag{9}$$

2.3. Proposed method based on deep learning and RLS algorithms

The block diagram of the proposed deep learning and RLS based estimator and the control system is shown in figure 1. Field oriented control algorithm of the control system is implemented in the microcontroller. The reference operating speed (ω_r^*), parameters of the id and iq controllers are set in the "User interface" block on Matlab/Simulink. The output of the d- and q- axes current controllers ($\hat{v}_d^*, \hat{v}_q^*$), the measured d- and q- axes currents ($\hat{\imath}_d, \hat{\imath}_q$) and the measured electrical speed ($\hat{\omega}_{re}$) from the microcontroller are fed to the deep neural network model for training and predicting the compensated d- and q- axes voltages ($\hat{v}_{d,comp}, \hat{v}_{q,comp}$) in Matlab/Simulink. These compensated d- and q- axes voltages together with those signals from microcontrollers are sent to the RLS based estimator to identify the machine inductances ($L_{d,est}, L_{q,est}$).

The mathematical model of a RLS based estimator is:

$$y_k = \Phi_k^T x \tag{10}$$

where x is vector of the unknown parameters to be estimated; Φ_k and y_k denote the input and output of the system, respectively; k is the sample instant. The update rule for RLS is:

$$\begin{aligned} \hat{x}_{k+1} &= \hat{x}_k + G_{k+1}[y_{k+1} - \Phi_{k+1}^T\hat{x}_k] \\ G_{k+1} &= P_k\Phi_{k+1}^T\left[I\lambda + \Phi_{k+1}^T P_k\Phi_{k+1}\right]^{-1} \\ P_{k+1} &= (P_k - G_{k+1}\Phi_{k+1}^T P_k)/\lambda \end{aligned} \tag{11}$$

where I is the identity matrix; λ is the forgetting factor; G_k and P_k the gain and covariance matrices, respectively.
The RLS algorithm can be implemented to estimate d- and q-axes inductances, the corresponding model will be:

$$x = \begin{bmatrix} L_{q,est} \\ L_{d,est} \end{bmatrix}, \Phi = \begin{bmatrix} -\hat{\omega}_{re}\hat{\imath}_q & 0 \\ 0 & \hat{\omega}_{re}\hat{\imath}_d \end{bmatrix} \tag{12}$$

$$y = \begin{bmatrix} \hat{v}_d^* + \hat{v}_{d,comp} - R_s\hat{\imath}_d \\ \hat{v}_q^* + \hat{v}_{q,comp} - R_s\hat{\imath}_q - \psi_m\hat{\omega}_{re} \end{bmatrix} \tag{13}$$

As can be seen in equations (3), (6) and (8), the compensated d- and q- axes voltages ($\hat{v}_{d,comp}, \hat{v}_{q,comp}$) are nonlinearly dependent of the parameters of the voltage source inverter, such as voltage drop on the main switches and free-wheel diodes, which are normally not available. This paper proposed a feedforward neural network model to estimate the compensated d- and q- axes voltages ($\hat{v}_{d,comp}, \hat{v}_{q,comp}$) based on the output of the d- and q- axes current controllers ($\hat{v}_d^*, \hat{v}_q^*$), the measured d- and q- axes currents ($\hat{\imath}_d, \hat{\imath}_q$) and the measured electrical speed ($\hat{\omega}_{re}$). The mechanism of this approach is the non-linear mapping of five measured input variables from microcontroller with two output variables. Therefore, the offline training of the neural network must be implemented using the PMSM with known parameters including stator resistance, d- and q- axes inductances, and rotor flux linkage. These parameters are experimentally identified by using the offline standstill IEEE standard method shown in [3].

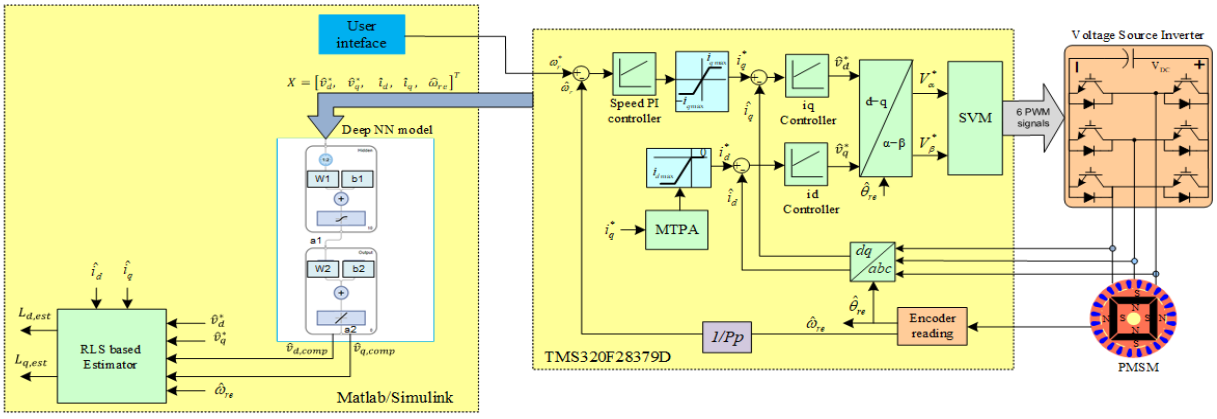

Figure 1: Block diagram of the proposed deep learning and RLS based estimator and control system.

As shown in (9), the output variables of the deep learning model can be calculated based on the measured input variables as follows:

$$\begin{aligned}\hat{v}_{d,comp}^{(training)} &= -\hat{v}_d^* + R_s\hat{\imath}_d + L_d\frac{d\hat{\imath}_d}{dt} - \hat{\omega}_{re}L_q \\ \hat{v}_{q,comp}^{(training)} &= -\hat{v}_q^* + R_s\hat{\imath}_q + L_q\frac{d\hat{\imath}_q}{dt} + \hat{\omega}_{re}(L_d\hat{\imath}_d + \psi_m)\end{aligned} \tag{14}$$

where $\hat{v}_{d,comp}^{(training)}$ and $\hat{v}_{q,comp}^{(training)}$ are compensated d- and q- axes voltages used to train to deep neural network model as the output variables.

The mathematic representation of every layer of the proposed feedforward neural network model shown in figure 1 is as follows:

$$\begin{aligned}a_1 &= tansig(W_1X + b_1) \\ a_2 &= purelin(W_2a_1 + b_2)\end{aligned} \tag{15}$$

where $X = \left[\hat{v}_d^*,\ \hat{v}_q^*,\ \hat{\imath}_d,\ \hat{\imath}_q,\ \hat{\omega}_{re}\right]^T$ is the input vector of the model; a_1, a_2 is the output of the hidden and output layer, respectively. a_2 is also the estimated compensated d- and q- axes stator voltages; W_1, b_1 and W_2, b_2 are weight, bias of the hidden and output layers, respectively.

The training data were collected by running the PMSM machine at different speeds from zero to rated value under different loading condition from no load to full load. The weight and bias metrices are updated using the Levenberg–Marquardt algorithm since this method can produce fast and stable convergence for the non-linear function [21]. The flow chart of the offline training process is presented in Figure 2 with the following steps [21].

- Step 1: Randomly initialize weights and bias matrices:

  $W_1[10\times 5], b_1[10\times 1], W_2[2\times 10], b_2[2\times 1].$

  In this study, the hidden layer was tested with a size of 10.

- Step 2: At every training epoch *k*, evaluate the mean square error (MSE) E_k.

$$E_k = \frac{1}{2}\sum_{i=1}^{2}\sum_{j=1}^{M} e_{ijk}^2 \tag{16}$$

$$e_{ijk} = a_{2,ijk} - \hat{a}_{2,ijk}$$

where M is the number of data set (70% of total data set); $\hat{a}_{2,ijk}$ is the output variable from the data set and calculated as shown in (14); $a_{2,ijk}$ is the estimated output variable from the neural network model as shown in (15).

- Step 3: Calculate the Jacobian matrices corresponding to weight and bias:

$$J_{W1,k} = \frac{\partial E_k}{\partial W_1} \qquad J_{W2,k} = \frac{\partial E_k}{\partial W_2}$$
$$J_{b1,k} = \frac{\partial E_k}{\partial b_1} \qquad J_{b2,k} = \frac{\partial E_k}{\partial b_2} \tag{17}$$

- Step 4: Update the weight and bias matrices.

$$\begin{aligned}W_{1,k+1} &= W_{1,k} - \left(J_{W1,k}^T J_{W1,k} + \mu I\right) J_{W1,k} e_k \\ W_{2,k+1} &= W_{2,k} - \left(J_{W2,k}^T J_{W2,k} + \mu I\right) J_{W2,k} e_k \\ b_{1,k+1} &= b_{1,k} - \left(J_{b1,k}^T J_{b1,k} + \mu I\right) J_{b1,k} e_k \\ b_{2,k+1} &= b_{2,k} - \left(J_{b2,k}^T J_{b2,k} + \mu I\right) J_{b2,k} e_k\end{aligned} \tag{18}$$

- Step 5: With the new weights and bias, evaluate the total error E_{k+1}.
- If the current total error is increased as a result of the update, then reset the weight and bias to the precious value) and increase combination coefficient μ by a factor of 10 and go back to step 4.
- If the current total error is decreased as a result of the update, then keep the new weight vector as the current one and decrease the combination coefficient μ by a factor of 10.
- Step 6: End the training if the total error is below the required value.

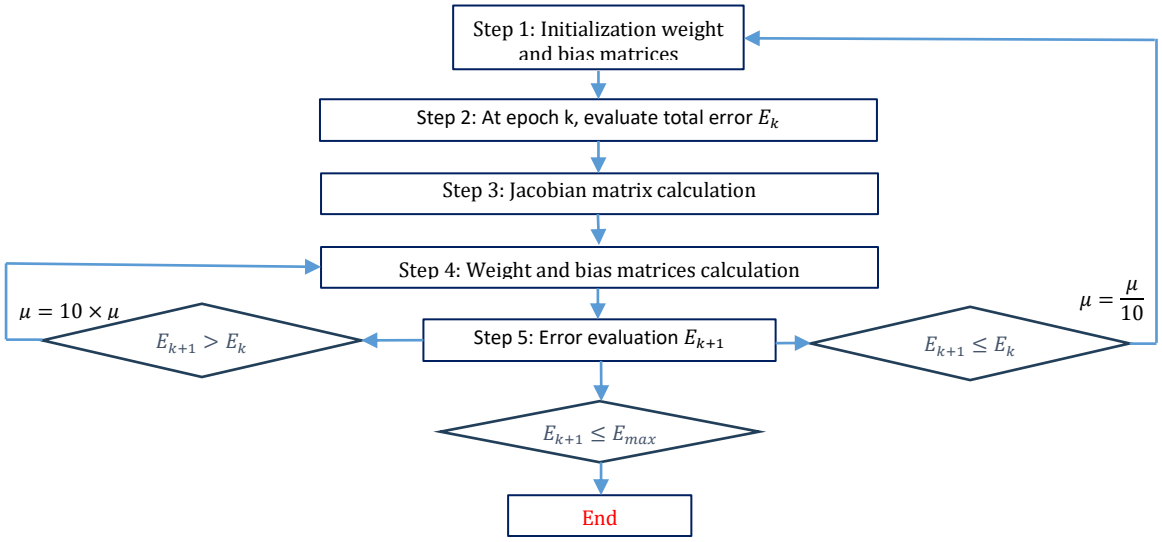

Figure 2: Flow chart of the offline training of the neural network for estimating the compensated d- and q- axes voltages.

3. Experimental validation

3.1 Experimental setup

The experimental setup is shown in figure 3. The tested PMSM's parameters are shown in Table I. The powder clutch ZKB0.6AN is used to load the tested PMSM. The three-phase two-level voltage source inverter, current sensing and DC voltage sensing circuits are integrated in the TI_IDDK_V2.2.1 evaluation module. The microcontroller TMS320F28379D-C2000-Delfino is used to implement the field-oriented control algorithm for the PMSM drive system. Matlab/Simulink and Code Composer Studio are used to compose and flash the program to the microcontroller. Matlab/Simulink are also used to implement the proposed parameter identification method, including the offline training and implementation of the deep neural network model for estimating the compensated d- and q- axes voltages, and realizing the RLS estimator for identifying machine inductances online.

Table1: Parameters of the teste PMSM (experiment)

Nominal Parameters	Value
L_d	0.0087 (H)
L_q	0.0087 (H)
ψ_m	0.063 (Wb)
R_s	2.25 (Ω)
Rated current (RMS)	2.7(A)
Rated torque	1.27 (Nm)
V_{DC}	300 (V)

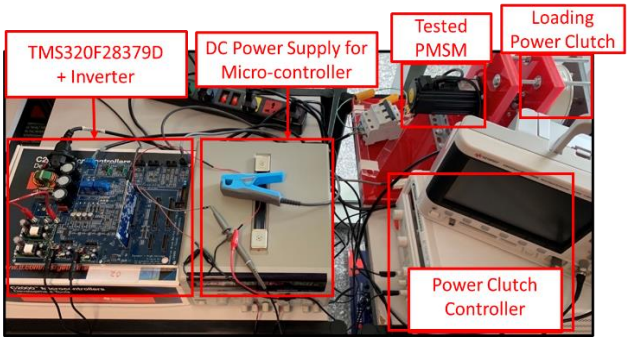

Figure 3: Experimental setup.

3.2 Offline training of the deep neural network using the experimental data

The feedforward neural network model for estimating the compensated d- and q- axes stator voltage was trained offline using the experimental data obtained by running the machine at different speed from zero to rated speed and loading conditions from no load to full load. The input and output data of 400000 samples are divided for the training, testing and validation by 70%, 15% and 15%, respectively. The hyper-parameters of the offline model training can be seen in Table II. The training statistic shown in figure 4 indicates that after 276 epochs, the mean square error (MSE) of the estimated and the actual compensated voltages is 0.0047. Further training accuracy can be achieved with larger training epochs.

Table 2: Hyper- Parameters of the offline training (experiment)

Parameter	Value
Size of hidden layers	10
Training Algorithm	Levenberg-Marquardt
μ	0.0001
Time delay	0.0001 (s)

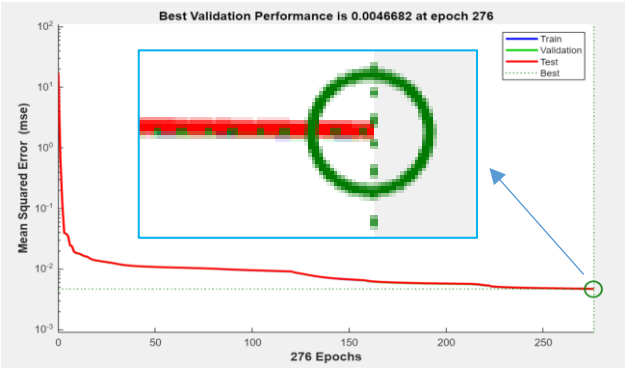

Figure 4. Training statistics of the neural network to estimate the compensated d-q axes stator voltage (experiment).

3.3. Experimental results

In order to evaluate the estimation accuracy and the robustness of the proposed parameter identification method against noise and effect of the non-linearity of the inverter, extensive experimental studies in various operation conditions of the control system were conducted. For the tested PMSM machine, the offline test shows that the machine inductances remain nearly unchanged over the loading range from no load to full load. Therefore, the armature reaction is negligible over the operating current range from zero to the rated value. Among all tested cases, the experimental results of the critical cases including the variation of the operating speed, load torque and field-weakening condition are presented as follows.

3.3.1. Variation of operating speeds

The performance of the proposed method under the variation of the operating speed is shown in figure 5. As can be seen in the first top subplot of figure 3, at time 4s the machine accelerates from 300 rpm to 1500 rpms, then decelerates to 900 rpm at time 8s. The measured d- and q-axes voltages (*vd meas* and *vq meas*) as the output of the corresponding id and iq current controllers in blue colors of the top second and third subplots vary according to the operating speeds. The compensation d- and q- axes voltages (*vd comp* and *vq comp*), which are sum of the compensated and the measured corresponding d- and q-axes voltages are shown in red color of the top second and third subplots. These compensation voltages also vary with the speeds and are deviated from the measured ones as the results of the proposed compensation scheme for the nonlinearity effect of the voltage source inverters. During the change of the operating speeds, the d-axis current was controlled at the value of -0.6A, and the light load was applied with q-axis current of 0.4A as can be seen in the subplot 4 and 5, respectively.

The comparison of the estimated (*Ld est* and *Lq est*) and the actual d- and q- axes inductances (*Ld actual* and *Lq actual*) are presented in subplot 6 and 7, respectively. It is clear that the estimated inductances follow closely with the actual ones of 8.7mH during the transient and steady states of the speed variations. The root mean square errors (RMSE) between the estimated and the actual d- and q- axes inductance over the whole period are 0.36 mH, 0.44 mH, respectively.

Discussion about the effect of the operation speed on the compensated d-axis voltage: Assume the expression of three phase currents as follows:

$$\begin{aligned} i_a &= I_m \cos(\hat{\theta}_{re}) \\ i_b &= I_m \cos(\hat{\theta}_{re} - \frac{2\pi}{3}) \\ i_c &= I_m \cos(\hat{\theta}_{re} + 2\pi/3) \end{aligned} \tag{19}$$

Assume the electric rotor angle $\hat{\theta}_{re}$ is between (0 to $\pi/3$), thus: $i_a > 0; i_b < 0; i_c > 0$

$$\rightarrow \left(\text{sign}(i_a), \text{sign}(i_b), \text{sign}(i_c)\right)^T = (1, -1, 1)^T \tag{20}$$

d- and q- axes voltage errors due to the inverter can be calculated as:

$$\begin{aligned} &\rightarrow \begin{pmatrix} \Delta\hat{v}_d \\ \Delta\hat{v}_q \end{pmatrix} \\ &= \frac{2}{3} U_{DB} \begin{pmatrix} \cos(\hat{\theta}_{re}) & \cos\left(\hat{\theta}_{re} - \frac{2\pi}{3}\right) & \cos\left(\hat{\theta}_{re} + \frac{2\pi}{3}\right) \\ \sin(\hat{\theta}_{re}) & \sin\left(\hat{\theta}_{re} - \frac{2\pi}{3}\right) & \sin\left(\hat{\theta}_{re} + \frac{2\pi}{3}\right) \\ \frac{1}{2} & \frac{1}{2} & \frac{1}{2} \end{pmatrix} \\ &\times \begin{pmatrix} 1 \\ -1 \\ 1 \end{pmatrix} \end{aligned} \tag{21}$$

$$\rightarrow \Delta\hat{v}_d = -\frac{4}{3} U_{DB} \cos\left(\hat{\theta}_{re} - \frac{2\pi}{3}\right) \tag{22}$$

Similarly, the d-axis voltage error can be calculated for other 60^o electric angle $\hat{\theta}_{re}$ between $\frac{\pi}{3}$ and 2π.

The average d-axis voltage error can be calculated as:

$$\begin{aligned} \Delta\bar{v}_d &= \frac{1}{\frac{\pi}{3}} \int_0^{\frac{\pi}{3}} -\frac{4}{3} U_{DB} \cos\left(\hat{\theta}_{re} - \frac{2\pi}{3}\right) \mathrm{d}(\hat{\theta}_{re}) \\ &= \frac{4\sqrt{3}}{\pi} U_{DB} \end{aligned} \tag{23}$$

If position measurement error ($\tilde{\theta}_{re}$) between the measured electric angle and the actual one is considered and $L_d = L_q$, the compensated d- axis voltage can be calculated as:

$$\hat{v}_{d,comp} = \Delta\hat{v}_d - \omega_{re}\psi_m sin\tilde{\theta}_{re} \tag{24}$$

Thus, the average compensated d-axis voltage can be calculated as:

$$\bar{v}_{d,comp} = \frac{4\sqrt{3}}{\pi} U_{DB} - \omega_{re}\psi_m sin\tilde{\theta}_{re} \tag{25}$$

It can be seen from equation (25) that the average compensated d-axis voltage $\bar{v}_{d,comp}$ is inversely proportional to the electrical speed ω_{re}. This can be verified by the experimental results shown in figure 5. To be specific, at the speed of 1500 rpm from 4 to 8s, the compensated d-axis voltage is about 0.5V, while at lower speed of 300 rpm from zero to 4s, the compensated d-axis voltage is much higher (about 3V). This explains why during the period from 0 to 4s, and from 4 to 8s the compensation d-axis voltage, which is the sum of the compensated and measured d-axis voltages, is relatively large compared to the measured one.

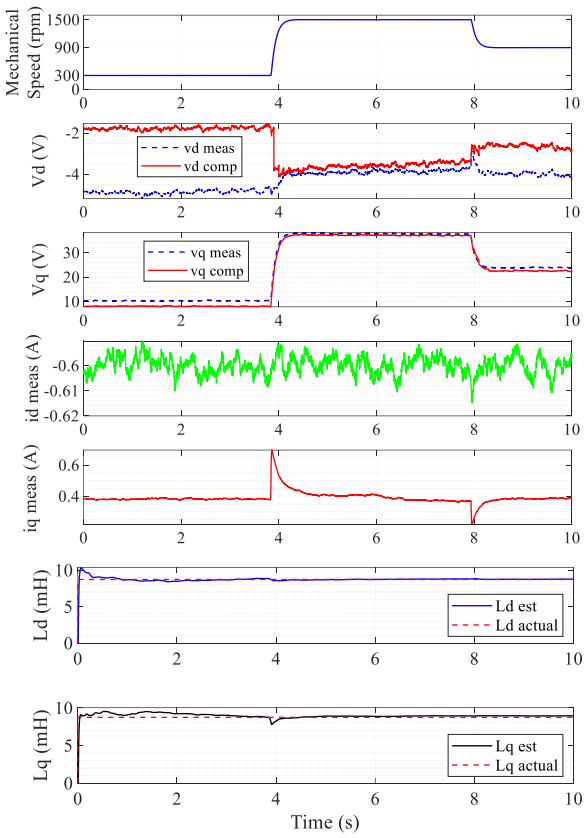

Figure 5. Estimation performance under the variation of the operating speeds (experiment).

3.3.2. Variation of load torque

The performance of the proposed methods with the variation of the load torque between light and full load under the operating speed of 300 rpm is shown in figure 6. The arrangement of the subplots of figure 6 is the same as for figure 5. As can be seen in the fifth subplot of figure 6, the load torque of the machine was changed between light to full loads at time 2s and 6.5s with the corresponding change of the q- axis current between 0.4A to 2.5A. It is worth mentioning that d-axis current is unchanged at -0.6A during the variation of the load torque as shown in the fourth subplot. As shown in the second and third subplots, the compensation d- and q- axes voltages are deviated from the measured d- and q- axes voltages as the results of the proposed compensation method.

The voltage difference between the measured and the computation vd is proportional to the operating current iq. This can be explained based on equations (6) and (25).

Equation (25) shows that the compensated vd ($\bar{v}_{d,comp}$) is proportional to U_{DB}. In addition, based on equation (6), U_{DB} is nearly proportional to the voltage drop on the main switch (V_S), since the term $\frac{T_{DB}+T_{on}-T_{off}}{T_{PWM}} \ll 0.5$. Furthermore, the V_S is nearly proportional to the operating current (iq) since the main switch (MOSFET) can be treated as a resistor.

It is clear in subplot 6 and 7 that the estimated inductances are closely matched with the actual ones of 8.7mH during the transient and steady states of the load torque variations. The RMSE between the estimated and the actual d- and q- axes inductances over the whole period are 0.51 mH, 0.64 mH respectively.

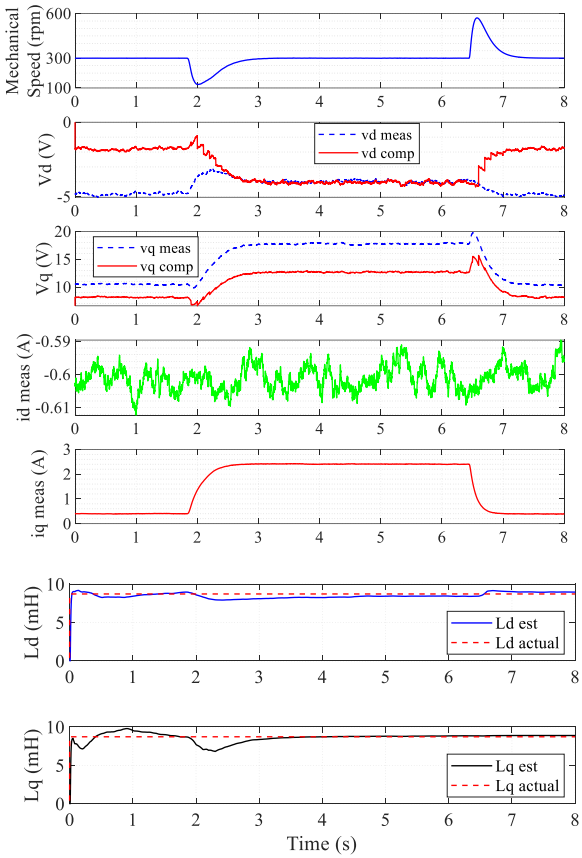

Figure 6. Estimation performance under the variation of the load torques (experiment).

3.3.3. Variation of field-weakening conditions

The performance of the proposed methods with the variation between light and heavy field-weakening condition under the operating speed of 300 rpm is shown in figure 7. As can be seen in the fourth subplot of the figure 6, at time 7.8s, the field-weakening was changed from light to heavy condition with the d-axis current change from -0.6A to -1.8A. As a result, the operating drops from 300 rpm to about 270 rpms as shown in the first subplot and the q-axis current is slightly increased from 0.4A to 0.6A. Subplots 2 and 3 also show the deviation of the measured and the compensation d- and q- axes voltages as the results of the proposed compensation scheme.

Subplots 6 and 7 clearly demonstrate that the estimated inductances are closely matched with the actual ones of 8.7mH during the transient and steady states of the field weakening variations. The RMSE between the estimated and the actual d- and q- axes inductances over the whole period are 0.39 mH, 0.68 mH respectively.

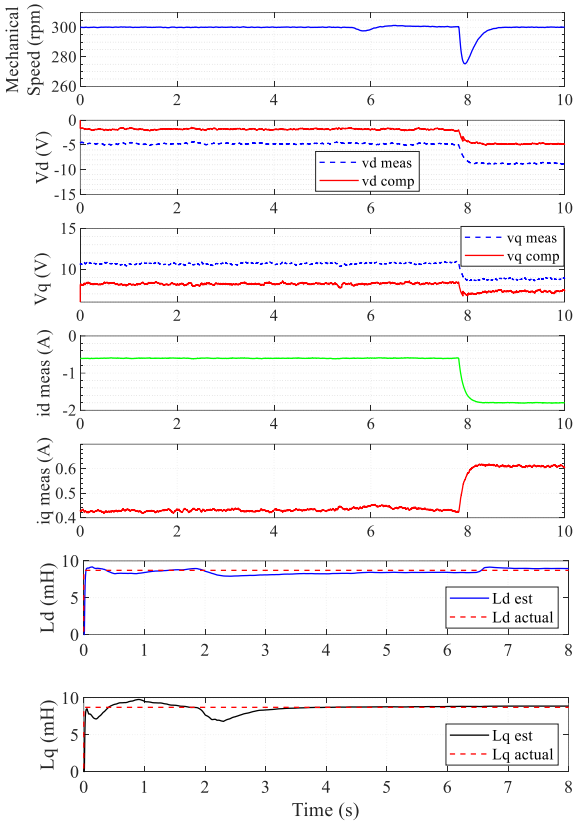

Figure 7. Estimation performance under the variation of the field-weakening conditions (experiment).

3.3.4. Comparison with conventional RLS-based method.

The comparison of the proposed method and the RLS-based method shown in [4] in terms of estimation accuracy was implemented by running the machine at the speed of 1500 rpm under light load condition. The experimental results of this study are shown in figure 8. The top subplot of the figure shows the measured operation mechanical speed around 1500 rpm. The second and third top subplots show the measured d- and q- voltages (*vd meas, vq meas*) in blue and the compensation d- and q- axes voltages (*vd comp, vq comp*) in red, which are the sum of the measured and the compensated ones. The fourth and fifth subplots present the operating d- and q- axes currents, respectively. Finally, the last two subplots present the actual inductances (*Ld actual, Lq actual*) in red, estimated inductances by the proposed method (*Ld est proposed, Lq est proposed*) in blue and the estimated inductances of the conventional RLS based method (*Ld est uncomp, Lq est uncomp*) in green.

It is obvious that the proposed method produces higher accuracy compared to the RLS based method. Specifically, the RMSE between the estimated and the actual d- axis inductances over the whole period of the proposed method

is 0.4 mH, while the RMSE of the RLS-based method was significantly higher (2.85 mH). Similarly, the RMSE between the estimated and the actual q- axis inductances over the whole period of the proposed method is 0.38 mH, while the RMSE of the RLS based method was higher (0.44 mH). The better estimation accuracy of the proposed method compared to the RLS-based method is due to the fact that the proposed method accurately compensates for the voltage errors caused by the voltage source inverter. In contrast, the RLS-based method does not consider the non-linearity effect of the inverter and it is only robust when the non-linearity effect of the inverter is negligible.

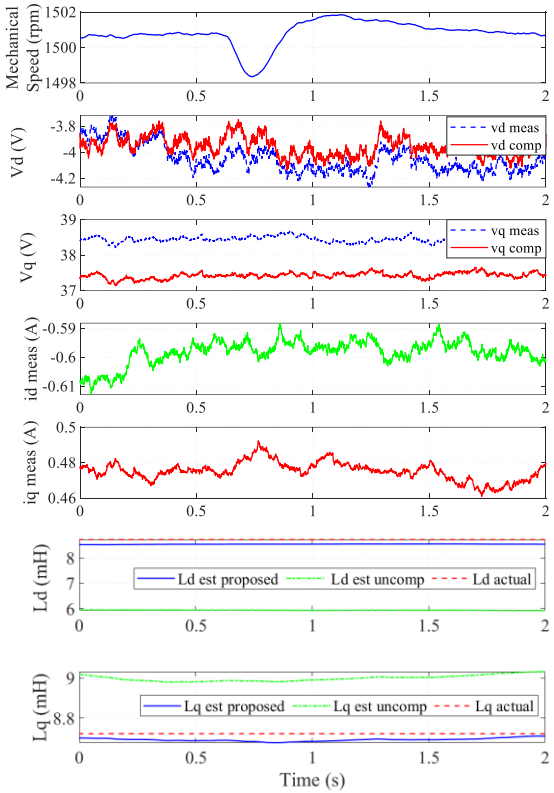

Figure 8. Performance comparison of the proposed and the uncompensated methods shown in [4] (experiment).

4. Conclusion

This paper has presented a novel approach to identify in real time d- and q- axes inductances of the PMSM based on the combination of deep learning and recursive least square algorithms. The deep learning model was proposed and trained offline using the experimental data to compensate the non-linearity of the voltage source inverter and the position measurement error, while the recursive least square algorithm was utilized to estimate d- and q- axes inductances based on the measured d- and q-axes currents, compensation d- and q- axes voltages and the operating speed. The proposed method overcomes challenges of the existing model-based estimators known as the effect of position measurement error and the requirement of accurate information of the inverter. The experimental results have demonstrated high estimation accuracy and the robustness of the proposed technique under various operating conditions including the variation of operating speed, load torque and field-weakening conditions. The experimental results also demonstrate the superiority of the proposed method, compared to the conventional RLS-based one.

Acknowledgement

This work was partly supported by the Nafosted Vietnam under the grant 107.99-2019.341.

References

[1] B. Ding, K. Huang, C. Lai, and G. Feng, "Correlated Inductance Modeling and Estimation of Permanent Magnet Synchronous Machines Considering Magnetic Saturation," *IEEE Transactions on Power Electronics*, vol. 38, no. 11, pp. 14463-14474, 2023, doi: 10.1109/TPEL.2023.3307715.

[2] *Rotating Electrical Machines Part 4: Methods for Determining Synchronous Machine Quantities From Tests*, IEC60034-4, 2008.

[3] "IEEE Guide for Test Procedures for Synchronous Machines Part I—Acceptance and Performance Testing Part II—Test Procedures and Parameter Determination for Dynamic Analysis - Redline," *IEEE Std 115-2009 (Revision of IEEE Std 115-1995) - Redline*, pp. 1-219, 2010, doi: 10.1109/IEEESTD.2010.5953453.

[4] S. J. Underwood and I. Husain, "Online Parameter Estimation and Adaptive Control of Permanent-Magnet Synchronous Machines," *IEEE Transactions on Industrial Electronics*, vol. 57, no. 7, pp. 2435-2443, 2010, doi: 10.1109/TIE.2009.2036029.

[5] S. Morimoto, M. Sanada, and Y. Takeda, "Mechanical Sensorless Drives of IPMSM With Online Parameter Identification," *IEEE Transactions on Industry Applications*, vol. 42, no. 5, pp. 1241-1248, 2006, doi: 10.1109/TIA.2006.880840.

[6] Y. Inoue, Y. Kawaguchi, S. Morimoto, and M. Sanada, "Performance Improvement of Sensorless IPMSM Drives in a Low-Speed Region Using Online Parameter Identification," *IEEE Transactions on Industry Applications*, vol. 47, no. 2, pp. 798-804, 2011, doi: 10.1109/TIA.2010.2101994.

[7] C. Lian, F. Xiao, J. Liu, and S. Gao, "Parameter and VSI Nonlinearity Hybrid Estimation for PMSM Drives Based on Recursive Least Square," *IEEE Transactions on Transportation Electrification*, vol. 9, no. 2, pp. 2195-2206, 2023, doi: 10.1109/TTE.2022.3206606.

[8] X. Li and R. Kennel, "General Formulation of Kalman-Filter-Based Online Parameter Identification Methods for VSI-Fed PMSM," *IEEE Transactions on Industrial Electronics*, vol. 68, no. 4, pp. 2856-2864, 2021, doi: 10.1109/TIE.2020.2977568.

[9] Y. Shi, K. Sun, L. Huang, and Y. Li, "Online Identification of Permanent Magnet Flux Based on Extended Kalman Filter for IPMSM Drive With Position Sensorless Control," *IEEE Transactions on Industrial Electronics*, vol. 59, no. 11, pp. 4169-4178, 2012, doi: 10.1109/TIE.2011.2168792.

[10] X. Xiao, C. Chen, and M. Zhang, "Dynamic Permanent Magnet Flux Estimation of Permanent Magnet Synchronous Machines," *IEEE Transactions on Applied Superconductivity*, vol. 20, no. 3, pp. 1085-1088, 2010, doi: 10.1109/TASC.2010.2041435.

[11] K. Liu, Z. Q. Zhu, Q. Zhang, and J. Zhang, "Influence of Nonideal Voltage Measurement on Parameter Estimation in Permanent-Magnet Synchronous Machines," *IEEE Transactions on Industrial Electronics*, vol. 59, no. 6, pp. 2438-2447, 2012, doi: 10.1109/TIE.2011.2162214.

[12] T. Boileau, N. Leboeuf, B. Nahid-Mobarakeh, and F. Meibody-Tabar, "Online Identification of PMSM Parameters: Parameter Identifiability and Estimator Comparative Study," *IEEE Transactions on Industry Applications*, vol. 47, no. 4, pp. 1944-1957, 2011, doi: 10.1109/TIA.2011.2155010.

[13] X. Yao, S. Huang, J. Wang, H. Ma, G. Zhang, and Y. Wang, "Improved ROGI-FLL-Based Sensorless Model Predictive Current Control With MRAS Parameter Identification for SPMSM Drives," *IEEE Journal of Emerging and Selected Topics in Power Electronics*, vol. 11, no. 2, pp. 1684-1695, 2023, doi: 10.1109/JESTPE.2022.3230700.

[14] K. Liu and Z. Q. Zhu, "Position-Offset-Based Parameter Estimation Using the Adaline NN for Condition Monitoring of

Permanent-Magnet Synchronous Machines," *IEEE Transactions on Industrial Electronics*, vol. 62, no. 4, pp. 2372-2383, 2015, doi: 10.1109/TIE.2014.2360145.

[15] Z. Wang, J. Chai, X. Xiang, X. Sun, and H. Lu, "A Novel Online Parameter Identification Algorithm Designed for Deadbeat Current Control of the Permanent-Magnet Synchronous Motor," *IEEE Transactions on Industry Applications*, vol. 58, no. 2, pp. 2029-2041, 2022, doi: 10.1109/TIA.2021.3136807.

[16] Z. Q. Zhu, D. Liang, and K. Liu, "Online Parameter Estimation for Permanent Magnet Synchronous Machines: An Overview," *IEEE Access*, vol. 9, pp. 59059-59084, 2021, doi: 10.1109/ACCESS.2021.3072959.

[17] K. Choi, Y. Kim, S. K. Kim, and K. S. Kim, "Auto-calibration of position offset for PMSM drives with uncertain parameters," *Electronics Letters*, vol. 56, no. 20, pp. 1048-1051, 2020/09/01 2020, doi: 10.1049/el.2020.1669

[18] M. X. Bui, "Online Parameter Identification Method using Neural Network for IPMSM," in *2022 25th International Conference on Electrical Machines and Systems (ICEMS)*, 29 Nov.-2 Dec. 2022 2022, pp. 1-6, doi: 10.1109/ICEMS56177.2022.9983070.

[19] M. X. Bui, D. Xiao, and M. F. Rahman, "Sensorless Control and Inductances Estimation of IPMSMs Using FPGA and High Bandwidth Current Measurement," *IEEE Access*, vol. 11, pp. 67322-67329, 2023, doi: 10.1109/ACCESS.2023.3287220.

[20] M. X. Bui, M. F. Rahman, D. Guan, and D. Xiao, "A New and Fast Method for On-line Estimation of d and q Axes Inductances of Interior Permanent Magnet Synchronous Machines Using Measurements of Current Derivatives and Inverter DC-Bus Voltage," *IEEE Transactions on Industrial Electronics*, vol. 66, no. 10, pp. 7488-7497, 2019, doi: 10.1109/TIE.2018.2883274.

[21] H. Yu and B. M. Wilamowski, "Levenberg–marquardt training," in *Intelligent systems*: CRC Press, 2018, pp. 12-1-12-16.